Low operational temperature Li–CF$_x$ batteries using cathodes containing sub-fluorinated graphitic materials

Jay Whitacre [a,*], Rachid Yazami [b], André Hamwi [c], Marshall C. Smart [a],
William Bennett [d], G.K. Surya Prakash [e],
Thomas Miller [c], Ratnakumar Bugga [a]

[a] *Jet Propulsion Laboratory, California Institute of Technology, Pasasdena, CA, United States*
[b] *CNRS, California Institute of Technology, Pasadena, CA, United States*
[c] *Université Blaise Pascal de Clermont-Ferrand, 63177 Aubière, France*
[d] *Glenn Research Center, Cleveland, OH, United States*
[e] *University of Southern California, Los Angeles, CA, United States*

Abstract

Commercial lithium/polycarbon monofluoride batteries [Li–(CF)$_n$] are typically current-limited and are therefore not implemented in high-rate or low-temperature applications. Recent results suggest, however, that CF-based cathodes that use sub-fluorinated CF$_x$ (SFCF$_x$) active materials in a thin electrode form factor are able to support very high currents (up to 5 C) while still providing a significant fraction of their specific capacity. In this work, the low temperature efficacy of these materials is examined in a −40 °C environment. CF$_{0.54}$ and CF$_{0.65}$ powders were characterized using X-ray diffraction, scanning electron microscopy, and X-ray energy dispersive spectroscopy. These materials were then implemented in a spray-deposited electrode using a 1-mil (∼25 µm) aluminum foil current collector and PVDF as a binder. Electrochemical tests showed that these materials were able to deliver specific capacity values up to five times greater than commercial CF$_{1.08}$ powder inserted into identically fabricated test cells tested at −40 °C. Testing also indicated that a room-temperature pre-discharge step was necessary to condition the electrode materials before exposure to the low-temperature test environment.
© 2006 Published by Elsevier B.V.

Keywords: CF$_x$ primary batteries; Low temperature; Sub-fluorinated CF$_x$; High rate; Electrode passivation

1. Introduction

There is a need for safe, high energy density primary batteries that can function at low temperatures, −40 °C and below, for a host of NASA (and other) applications. The existing off-the-shelf suite of batteries capable of providing energy at reasonable rates at these temperatures, including Li–SO$_2$Cl$_2$, Li–MnO$_2$, and Li–SO$_2$ have lingering safety issues or low temperature energy density values that make the further investigation of new low temperature battery chemistries justifiable. The high energy density and inherently safe nature of the Li–CF$_x$ electrochemical couple make it very appealing, though this chemistry is thought to be severely rate limited, particularly at low temperatures. It was our intention, therefore, to explore the possibility of creating high rate (C/10 to C/20) Li–CF$_x$-based batteries that can function well in environments no warmer than −40 °C, while still providing high energy density. In doing so, we examined the performance of sub-fluorinated CF$_x$ materials as implemented in a thin electrode form factor.

Commercial Li/CF$_x$ batteries can deliver up to 700 Wh kg^{-1}, 1000 Wh l^{-1} (at room temperature, C/100 rate) and typically use active cathode materials consisting of fluorinated carbonaceous materials such as coke or graphite [1,2]. These cathodes have compositions typically ranging from CF$_{1.05}$ to CF$_{1.1}$ that can deliver specific capacities in excess of 800 mAh g^{-1} at 2.5 V under low-rate conditions at room temperature [3]. This cathode material, however, is known to be discharge rate limited, and currents lower than C/50 (battery current 1/50th

that of the capacity of the battery divided by 1 h) are often necessary to avoid cell polarization and large capacity loss. Oftentimes, the low electronic conductivity of CF is cited as the cause of the observed discharge rate limitations, and it has been long been known that there is a strong correlation between cathode thickness and performance; thicker cathodes are prone to be more rate-limited [4]. To this end, a number of Li–CF$_x$ battery manufacturers, have been developing high-rate CF$_x$ cells that use thin cathode structures in a spirally wound configuration. Some very promising results have been recently described, including a 15.5 Ah fully packaged D cell that delivers over 460 Wh kg^{-1} at better than a C/8 rate [1]. At $-20\,°$F ($-29\,°$C), these same cells delivered about 12 Ah under a 2 A discharge, with an active cathode materials utilization of over 570 mAh g^{-1}. A similar electrode design approach developed had a bulk cathode impedance of 0.0002 Ω mm^{-2} and was able to deliver over 500 mAh g^{-1} active cathode material at a C/20 rate at $-30\,°$C [5]. Others have reported that the Li–CF$_x$ chemistry exhibits substantial self-heating under some discharge conditions [6]. While this is a liability at ambient or elevated temperature use, properly designed cells and batteries could take advantage of this effect for very low temperature operation.

To examine the possibility of further augmenting these results, we have taken advantage of the relatively high electronic conductivity sub-fluorinated CF$_x$ (SFCF$_x$) cathode materials [4,7,8]. Recently, substantial success has been reported wherein CF$_x$ with $0.3 < x < 0.8$ has been used in test cells that are capable of discharge rates as high as $5C$ at room temperature with excellent capacity retention [8]. It was unknown, however, whether these cathodes would possess the same characteristics at very low temperatures or high rates. This is because it is possible that significantly slower cathode reaction kinetics and lower ion conductivity values at these temperatures could mitigate the benefits observed at room temperature for the enhanced electronic conductivity SFCF$_x$ materials. Furthermore, the factors that cause the well-known voltage delay effect in Li–(CF)$_n$ batteries are likely to be more prominent under high-rate, low temperature conditions and so must be examined and understood if a functional battery is to be eventually produced. The following describes the performance of Li–CF$_x$ test cells based on SFCF$_x$ active cathode materials and electrolytes designed to function well at low-temperatures. A series of test cells based on commercially supplied CF$_{1.08}$ powders were tested in parallel in identical test cells.

2. Experimental

2.1. Materials fabrication and analyses

Sub-fluorinated CF$_{0.54}$ and CF$_{0.65}$ cathode materials were produced as described elsewhere [8]. A monel boat, containing Madagascar natural graphite (30 g) with average particle size of about 10 μm, was placed in a nickel reactor and heated under pure fluorine gas flow at 375 and 390 °C during 17 h to produce CF$_{0.54}$ and CF$_{0.65}$, respectively. The products and were analyzed using X-ray diffraction (Cu Kα radiation), scanning electron microscopy (SEM) and X-ray energy dispersive spectroscopy (XEDS).

2.2. Electrochemical analyses

Spray-deposited cathodes were fabricated using SFCF$_x$ powders that were prepared using a mix consisting of 80, 10 wt.% carbon black in a NMP solution solvating 10 wt.% PVDF (pre-stirred solution). As a control, a commercial CF$_{1.08}$-based cathode mixture was also produced which had a similar overall fluorine mass fraction as in the CF$_{0.54}$ mix (and so therefore had a higher carbon-diluent-to "active material" ratio). Specifically, these baseline cathodes contained 30 wt.% C black, 60 wt.% CF$_{1.08}$ and 10 wt.% PVDF. In all cases the fully intermixed slurry (as mechanically stirred for at least 12 h) was spray-deposited in multiple layers onto a roughened 1-mil thick Al foil current collector. The resulting physically robust cathode structures, 1–3 mil in thickness, were vacuum-furnace dried for 24–48 h at $\sim$105 °C. 2032 size coin cell test cells were then fabricated using 16 mm diameter cathode disks, a single layer of Tonen separator, and a 16 mm diameter Li foil anode.

The electrolytes contained 1 M LiBF$_4$ salt solvated in a mix of either propylene carbonate (PC) + 1,2,-dimethoxy ethane (DME) in a 20/80 or 50/50% (v/v) ratio. Since these electrodes were so thin, the variation in wettability between these two solvent compositions was not found to have a significant effect on cell performance. A series of electrolytes made using various solvent additives has also been performed, and will be reported on elsewhere in detail.

Electrochemical testing consisted of galvanostatic discharges at room temperature and $-40\,°$C under currents consistent with rates ranging from $2C$ to C/40. These rate values were calculated using the nominal room-temperature specific capacities that have been previously published for these SFCF$_x$ materials. A room-temperature pre-discharge step of 3% of the total estimated cathode capacity at a C/33 rate was employed in most cases. Electrochemical impedance spectroscopy (EIS) in the potentiostatic mode (5 mV signal amplitude, 10^{-2} to 10^5 Hz frequency range) was carried out to examine the effect of this pre-discharge on the cathode an anode.

3. Results

3.1. Materials characterization

Fig. 1 show X-ray diffraction data collected from the SFCF$_x$ materials for $x = 0.54$ and 0.64. These data show that both pristine graphite as well as fluorinated CF materials were present. There was more graphitic C in the CF$_{0.54}$ than in the CF$_{0.64}$, and there is no evidence of staging in the fully unfluorinated material (the graphite peak is at the same location for both cases). The broad diffraction peaks from the fluorinated material present in the samples are similar in both of the SFCF$_x$ materials and are consistent with those found in carbon materials that have been uniformly fluorinated to approximately CF$_{0.8}$ [9].
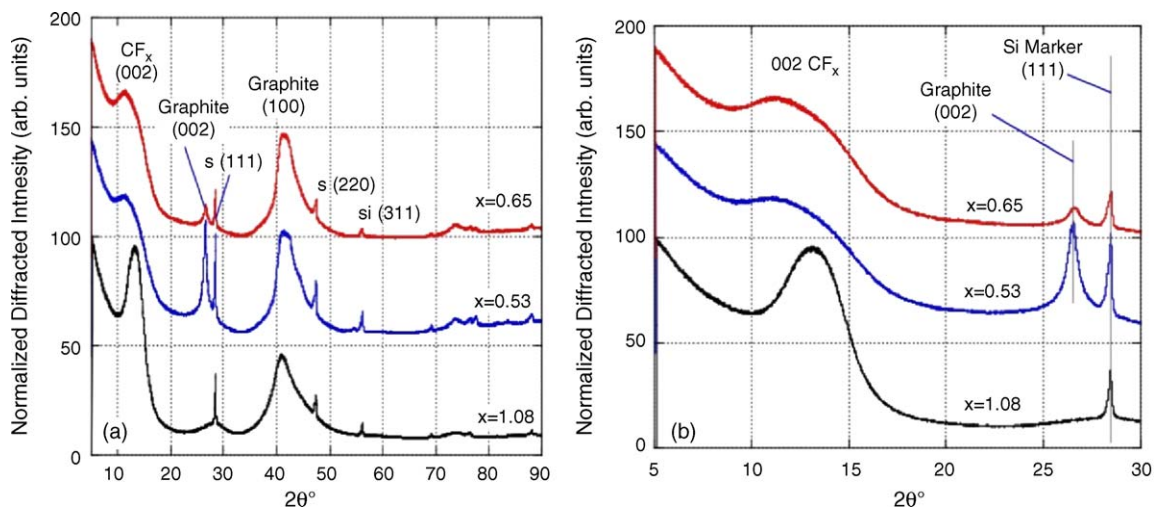
Fig. 1. X-ray diffraction patterns (Cu Kα radiation) from the two different SFCF$_x$ materials studied.

Scanning electron micrographs of this material are shown in Fig. 2. The powders consisted of flakes of material varying in size from less than 1 μm to over 10 μm in diameter. The flakes had a similar morphology as unfluorinated graphite. Fig. 3 contain XEDS elemental mapping data of the CF$_{0.54}$ material. These data show that the C and F atoms in the material are generally well mixed such that the F signal is observed on each C flake (Fig. 4). Fig. 5 is a long-acquisition time elemental XEDS line scan indicating, once again, that the F is fully and equally dispersed in the graphitic flakes. These data show that the CF$_x$ powder was not a mix of unfluorinated graphite particles mixed with fully fluorinated CF, but rather that each flake contained both unfluorinated graphite and CF$_y$.

3.2. Electrochemical characterization

3.2.1. Room-temperature characterization

To verify that these SFCF$_x$ materials were similar to those reported previously, a number of room-temperature discharges were conducted [8]. In these cases, the electrolyte consisted of either 1.0 M LiBF$_4$ in PC + DME (20/80 or 50/50% (v/v)). Fig. 5

shows the discharges of Li–CF$_{0.54}$ cells at room temperature at 2C and C/5 rates. The capacities realized from these cells are very similar to those reported earlier and indicate that these materials performed as expected.
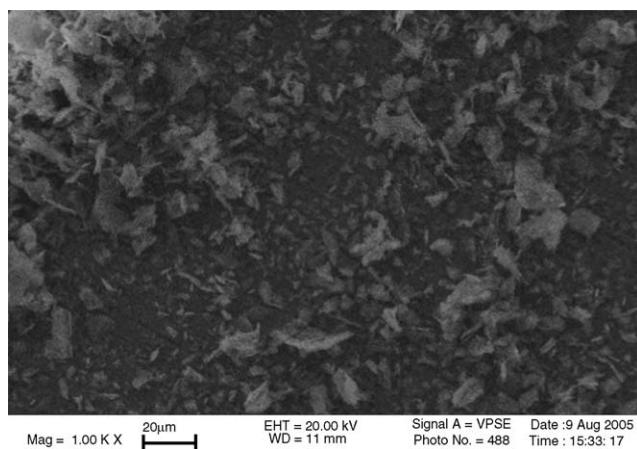

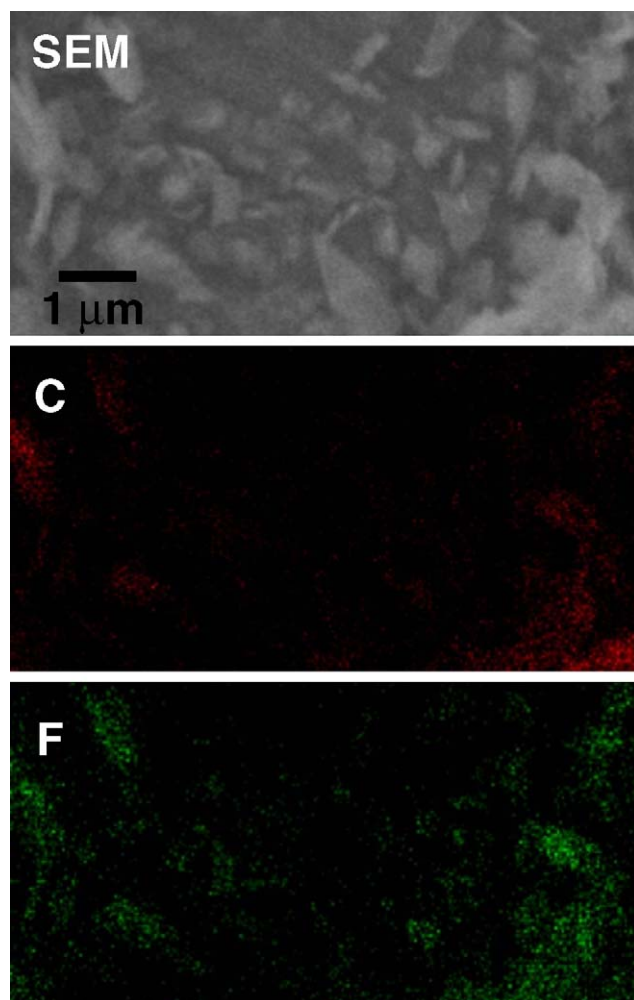Fig. 2. Scanning electron micrograph of pure CF$_{0.54}$ material dispersed on an Al sample holder.
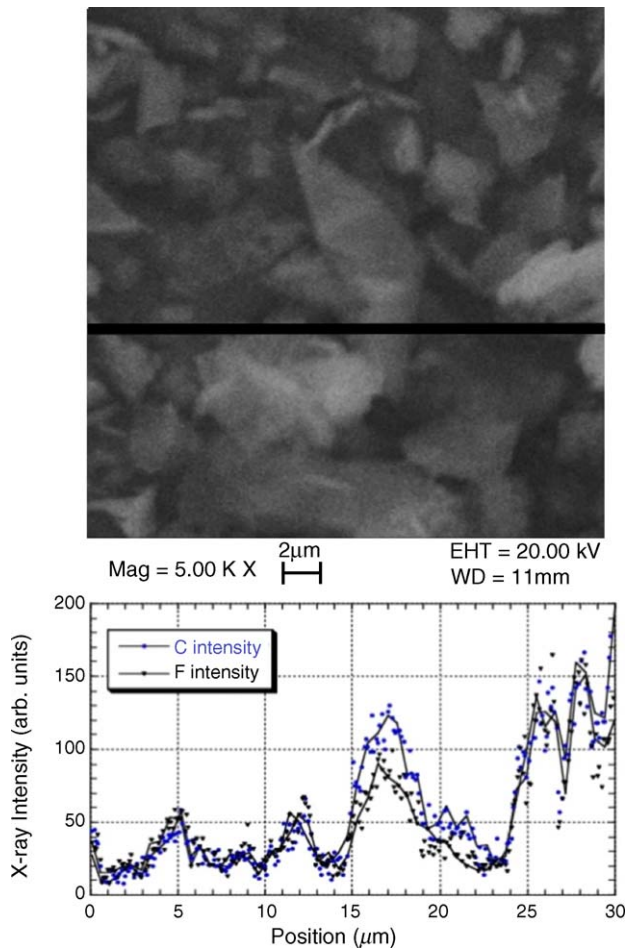
Fig. 3. SEM/XEDS mapping of CF$_{0.54}$ material.

Fig. 4. Line scan X-ray energy dispersive data showing the relative normalized intensities of the Kα X-rays excited as a function of position (as indicated by line on SEM image).

The baseline cathodes fabricated using commercial $CF_{1.08}$ and 30 wt.% carbon black material were also discharged at room temperature at high rates, as shown in Fig. 6. These materials delivered slightly higher specific capacities. In this case 80% of
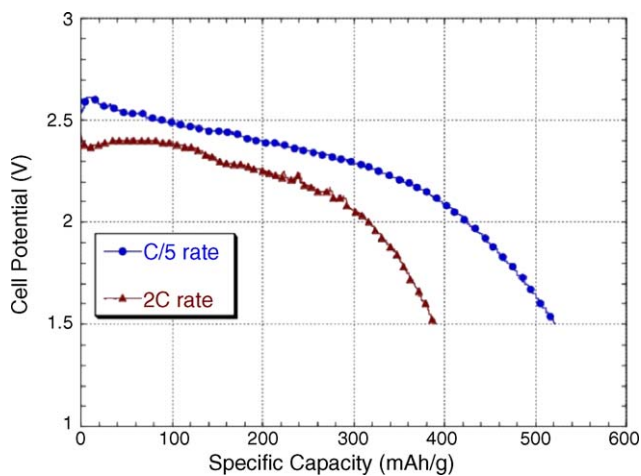

Fig. 5. Discharge profiles of $CF_{0.54}$ cathodes at room temperature at $2C$ and $C/5$ rates. These cathodes were approximately 1 mil in thickness, and contained 80 wt.% $CF_{0.54}$.
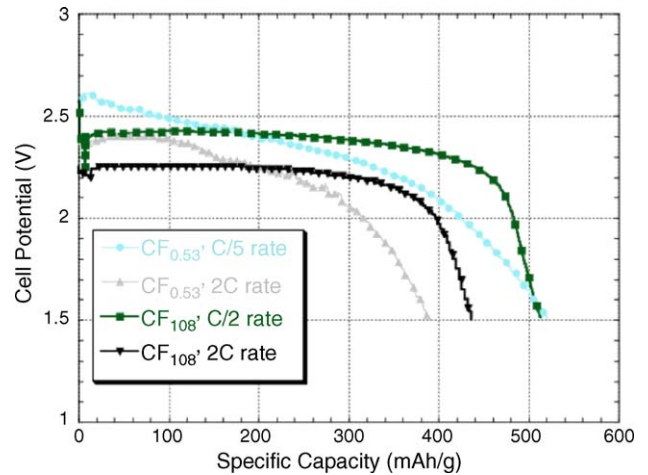

Fig. 6. Discharge data from cathodes made with a mix of a high-mass fraction schwanagan black and commercially fabricated $CF_{1.08}$ at $C/5$ and $2C$ discharge rates (data from the $CF_{0.54}$ materials are shown for comparison). The overall C/F ratio in these composite cathodes was similar as those in the $CF_{0.54}$ cathode mix.

the total cathode mass was defined as the "active material" mass to allow for a reasonable comparison with the $SFCF_x$ containing cathodes.

Room-temperature discharge data from a $CF_{0.65}$ cathode are shown in Fig. 7. These data are also consistent with previously published data: a specific capacity of over $700 \, \text{mAh g}^{-1}$ was obtained at a $C/5$ rate, with a discharge voltage in excess of 2.5 V. The initial voltage plateau was also more constant than in the $CF_{0.54}$-based cells.

3.2.2. Low temperature testing

Test cells made from the same materials as for the room-temperature testing were discharged at $-40\,^\circ$C. Fig. 8 shows
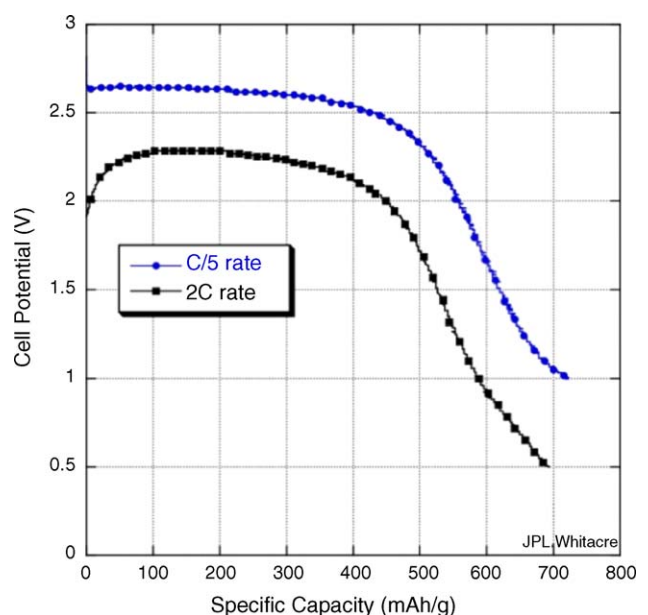

Fig. 7. Room-temperature data from a Li–$CF_{0.65}$ test cell. The cathodes were about 1.5 mil thick. Discharge rates were $C/5$ and $2C$.
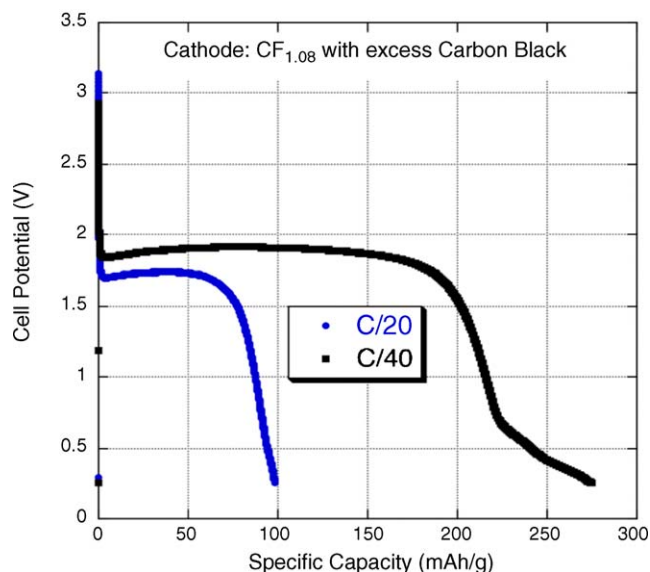
Fig. 8. Performance of the cathodes based on commercial $CF_{1.08}$ material mixed with 30 wt.% carbon black. The electrolyte solvent was 20/80 wt.% PC/DME, the discharge temperature was −40 °C, the active material mass was 6.08, 4.64 mg for the $C/20$, $C/40$ cells, respectively, and the cathode thickness: <1 mil.

the performance of the $CF_{1.08}$-based cathode material at −40 °C (using 20/80 PC/DME electrolyte solution) in two separate cells using $C/20$ and $C/40$ rates (with room-temperature pre-discharge). About 200 mAh g^{-1} was extracted at a $C/40$ rate, while less than 100 mAh g^{-1} was attained at a $C/20$ rate, results that are nominally consistent with those published previously for $CF_{1.08}$-based cathodes at low temperatures.

Fig. 9 shows the −40 °C performance of Li–$CF_{0.65}$ cells (using 20/80 PC/DME electrolyte solution) with and without the room-temperature pre-discharge step. A capacity of
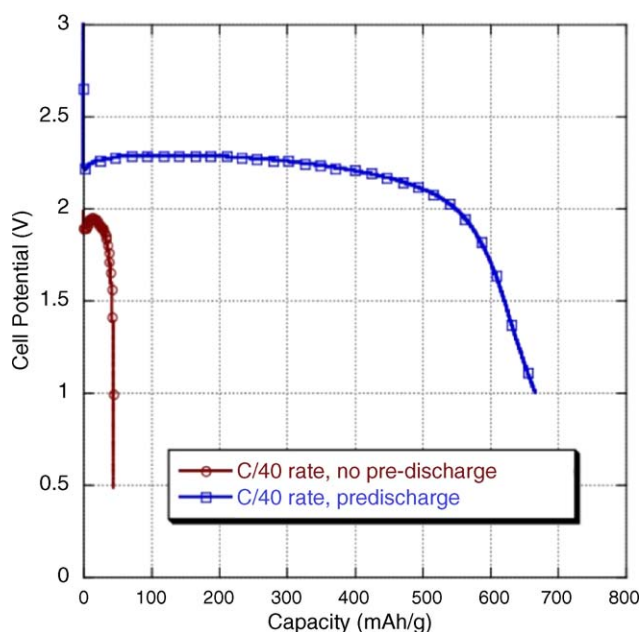

Fig. 9. Discharge data from similar Li–$CF_{0.65}$ test cells at −40 °C with and without a room-temperature pre-discharge of 3% the total capacity of the cell.

600 mAh g^{-1} was extracted from the cathode that had undergone the pre-discharge. This experiment was repeated several times using different electrolytes and cathode materials and the results were similar: the pre-discharge was necessary to render the cells effective at low temperatures. For this reason, this conditioning step was adopted and used for all testing.

Fig. 10 shows discharge curves from $CF_{0.65}$ and $CF_{0.54}$ cells at −40 °C, using multiple discharge rates in succession. In Fig. 10(a), a $CF_{0.65}$ and cell was first discharged at a $C/20$ rate (to 0.5 V) followed by a discharge at a $C/40$ rate, while in Fig. 10(b) the respective rates were $C/10$ and $C/20$ on a $CF_{0.65}$ cell. In this case, the total capacity delivered under a $C/20$ discharge current was greatly enhanced if preceded by a $C/10$ discharge. This effect was not observed in all cases, however, as can be seen in Fig. 11(c) showing the performance of Li–$CF_{0.54}$ under $C/10$ followed by $C/20$ discharge rates, where an inconsistent discharge potential was observed at a $C/10$ rate through 170 mAh g^{-1} of capacity. The $C/20$ discharge on the same cell was smooth and the cell provided a total of 460 mAh g^{-1}.

Table 1 contains a partial list of test cells, composition, test conditions, and resulting capacities.

4. Discussion

4.1. Microstructure

The characterization data indicate that the $SFCF_x$ materials were comprised of pristine unfluorinated graphite mixed intimately with fluorinated C, and are consistent with data reported previously. The SEM/XEDS analyses indicate that the C and F are intermixed at a very fine scale (at least smaller than tens of nm), while the XRD data show that the graphitic material that has undergone fluorination is likely fluorinated to the same degree regardless of the total fluorination of the sample (i.e. x in CF_x). There is also no evidence of graphitic gallery staging at the various levels of fluorination. The combination of these indicators suggests that the microstructure of this material is a collection of nano-dimensional graphite and CF_y domains, where y is approximately 0.8–0.9. The small scale of these compositionally variant regions dictates that the material have a very high graphite-to-CF_y surface area and subsequently will posses excellent electronic/interface transport properties at all temperatures.

Although thermodynamically predictable, the fluorination of graphite is kinetically unfavorable as it requires the following: (i) separation of the graphene layers to allow for fluorine diffusion, (ii) change in the carbon hybridization from stable sp^2 to less stable sp^3, and (iii) dissociation of the F_2 molecule. At constant temperature and fluorine pressure, the chemical activity of fluorine decreases with the depth of fluorine penetration within the layers. Consequently, the rate of the fluorination reaction ($C + y/2F_2 = CF_y$) should decrease as the diffusion layer becomes thicker, which eventually leads to an equilibrium state in which possibly a fraction of carbon remains unreacted. At 375 and 390 °C used to prepare $CF_{0.54}$ and $CF_{0.64}$ samples respectively, under 1 atm fluorine pressure, the practical end point is reached after 17 h reaction. Both samples show unreacted graphite.
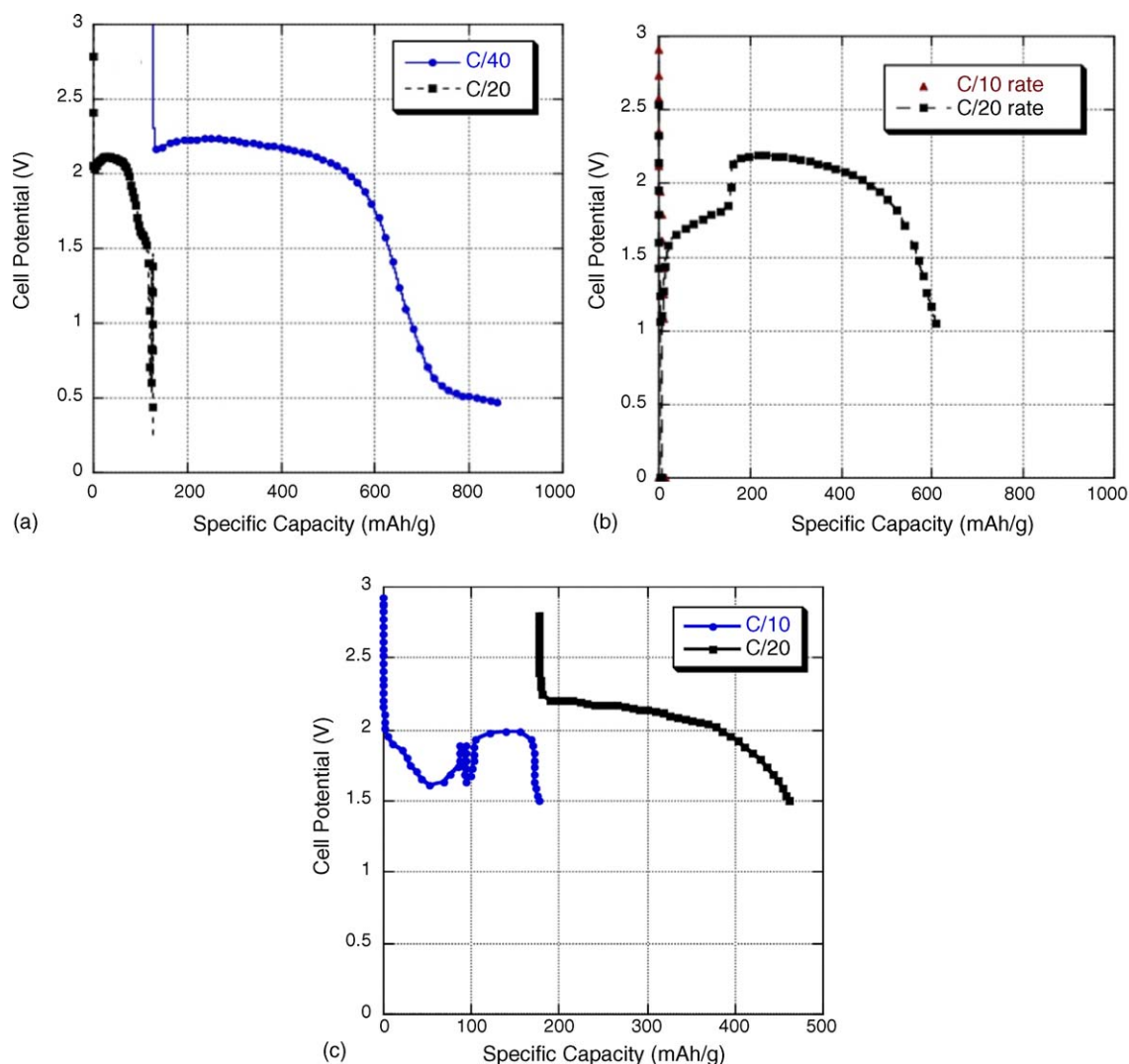
Fig. 10. Discharge data from test cells at $-40\,^\circ$C as discharged at different rates: (a) $CF_{0.65}$ test cell discharged at a $C/20$ rate followed by a $C/40$ rate; (b) $CF_{0.65}$ test cell discharged at a $C/10$ rate followed by a $C/20$ rate; (c) Li–$CF_{0.54}$ test cell at a $C/10$ rate followed by a $C/20$ rate at $-40\,^\circ$C.

4.2. Electrochemical behavior

To establish that this uniquely structured material offers some benefits compared to state-of-the-art $(CF)_n$ cathode materials, it was necessary to create a control cathode based on commercially available $CF_{1.08}$ that had the same fraction of fluorine in the as-tested cathode structure. Relatively large quantities of C black were used to lower the total F content in these cathodes to the same level as found in the $CF_{0.54}$-based cathodes (which used 10 wt.% carbon black). At room temperatures, there was little difference between the $SFCF_x$ material and the industry baseline, as seen in Fig. 6. Though the $CF_{0.54}$ material had a higher potential initially, this material had a discharge plateau that was more sloping, and actually delivered less capacity at room temperature than the $CF_{1.08}$ cathodes. This result is not unexpected, as the very thin cathode form factor used in these cells likely minimized the beneficial effects of the enhanced conductivity found in the $SFCF_x$ materials. It is possible that substantially thicker cathode structures would allow for the difference in performance between the $CF_{1.08}$ and the $CF_{0.54}$ to be resolved.

At $-40\,^\circ$C, however, the commercial $CF_{1.08}$ baseline and $SFCF_x$ cathode materials behaved differently. In particular, the $CF_{1.08}$ yielded significantly lower capacities at lower discharge potentials than the $SFCF_x$ materials, even though the latter were in a slightly thicker electrode form factor, as summarized in Table 1. The $CF_{1.08}$-based cathodes typically delivered one-third the capacity of the $CF_{0.65}$ material under identical conditions. The result is more pronounced when considering the fact that the baseline material cathodes also polarized to a greater degree, thereby offering an energy density.

This result indicates that *the nano-scale intermixing of graphitic and CF_y materials is critical for low-temperature performance*, and cannot be emulated by physically mixing high surface area carbon materials with $CF_{1.08}$ as which was shown to be sufficient for higher temperature testing environments. The two main differentiating features of the $SFCF_x$ material compared to the $CF_{1.08}$ were (1) higher surface-area-to-mass ratio for the active CF_y domains, and (2) the existence of nano-scale electronically conductive pathways. It is not yet known, however, which of these two (or both) physical characteristics played
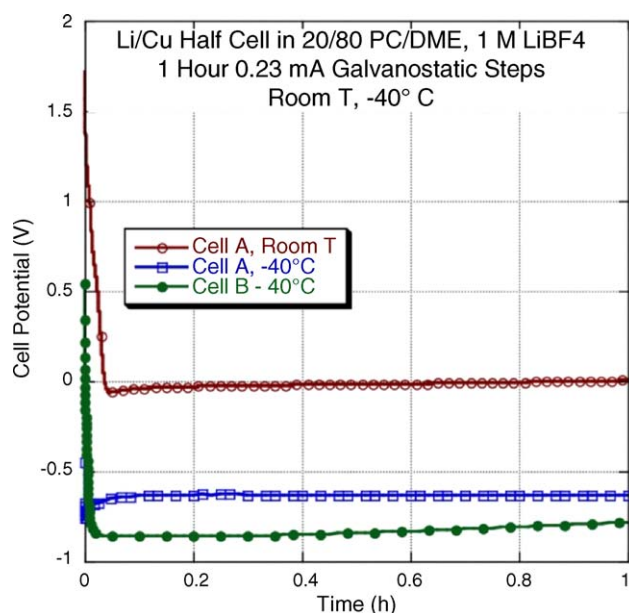
Fig. 11. Potential vs. time plots for room temperature and $-40\,°C$ galvanostatic testing on Li/Cu half cells. The current used, 0.23 mA, was a typical discharge rate for the Li–CF$_x$ cells.

the dominant role in increasing cathode performance at low temperatures. This mechanism is under study and will be directly addressed in future communications.

The capacity/energy density of a D-sized cell produced using the CF$_{0.647}$ cathode material can now be estimated (for a $-40\,°C$, $C/40$ discharge condition). It is assumed that the CF$_{0.647}$ active material may be inserted into the same cell structure the 15.5 Ah D-size LiCF$_x$ battery described in the introduction. Substituting 600 mAh g^{-1} CF$_{0.647}$ into this cell format results in a cell with

an energy density of about 400 Wh kg^{-1} when discharged at a $C/40$ rate at $-40\,°C$.

It was found that the low-temperature performance of all CF$_x$ materials was greatly enhanced if a small, room-temperature pre-discharge was used. This protocol is commonly used for industrially fabricated Li–CF$_x$ batteries to condition the electrode/electrolyte interfaces. The observed effect could have been a result of the existing native Li anode passivation layer of LiOH species that is removed with a short discharge, as has been suggested previously [10]. To examine this possibility, several Li half-cells (using Cu foil as a counter electrode) were constructed with the same electrolyte/salt/separator as used in the full Li–CF$_x$ cells. $-40\,°C$ galvanostatic electrochemical tests were conducted on cells that both had and had not been subjected to the room-temperature galvanostatic conditioning step identical to that used in the full cells. Fig. 11 shows the results: after a 1 h of discharge at $-40\,°C$, there was approximately a 0.15 V difference in the Li/Cu plating potential (under a galvanostatic condition) between the half cell that did and the half cell that did not undergo the room-temperature conditioning. The magnitude of this differential is significantly smaller than that observed for the full cells discharged and without room-temperature conditioning (as seen in Fig. 9).

Other tests using a flooded three-electrode glass cells indicated the same result. Fig. 12 shows the anode, cathode and full cell potential (versus Li reference electrode) as a function of time during a 2 h pre-discharge of a thick CF$_{1.08}$-based cathode. During the discharge, the anode polarizes approximately 5 mV, while the cathode potential varies though a range of nearly 1 V. EIS analyses on the cathode of this cell before and after the pre-discharge are conclusive (Fig. 13): the cathode interfacial resistance decreased to about 20%

Table 1

Partial list of test cells, discharge conditions, and specific capacity/energy values (as calculated based on cathode active material mass content). The capacity for those cells discharged using more than one rate is given as the sum of the capacities obtained (as indicated by the "+" signs)

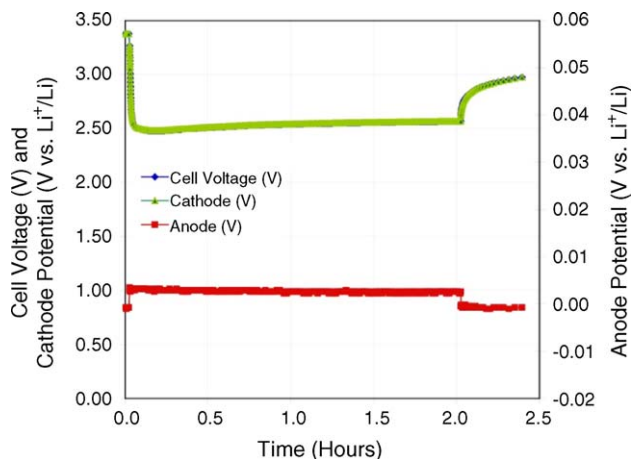| Cathode	Thickness (mil)	Temperature (°C)	Discharge rate	Capacity (mAh g^{-1})	Average potential (V)	Wh kg^{-1}
CF$_{1.08}$ with excess C	<1	20	2C	430	2.2	946
CF$_{1.08}$ with excess C	<1	20	C/2	510	2.4	1224
CF$_{1.08}$ with excess C	<1	−40	C/20	75	1.6	120
CF$_{1.08}$ with excess C	<1	−40	C/40	200	1.9	380
CF$_{0.53}$	∼1	20	C/5	510	2.5	1275
CF$_{0.53}$	∼1	20	2C	390	2.5	975
CF$_{0.53}$	∼1	−40	C/10	393	1.9	1127
			C/20	+59	2.1	+124
				443		1251
CF$_{0.53}$	∼1	−40	C/10	334	1.9	635
			C/20	+109	2.1	+228
				452		863
CF$_{0.647}$	∼2 to 3	20	C/5	600	2.6	1560
CF$_{0.647}$	∼2 to 3	20	2C	525	2.3	1207
CF$_{0.647}$	∼2 to 3	−40	C/40	630	2.25	1417
CF$_{0.647}$	∼1 to 2	−40	C/40	610	2.25	1372
CF$_{0.647}$	∼1 to 2	−40	C/40	615	2.25	1383
CF$_{0.647}$	∼2 to 3	−40	C/20	110	2.15	236
			C/40	+510	2.25	+1174
				620		1410
CF$_{0.647}$	∼2 to 3	−40	C/10	10	1.75	17
			C/20	+570	2.25	+1282
				580		1299

Fig. 12. Three-electrode measurements using a Li reference electrode on a Li–$CF_{1.08}$ glass test cell. The scale for the anode potential is on the right.

its pre-discharge value. These results are consistent with the idea that the voltage delay/pre-discharge effects are driven by cathodic mechanisms. It is possible that the pre-discharge encourages the formation of an unfluorinated C layer at the electrode/electrolyte interface as a result of the cathode process ($CF_x + \varepsilon Li^+ + \varepsilon e^- = \varepsilon LiF + \varepsilon/xC + (1 - \varepsilon/x)CF_x$). Such an in situ formed layer would enhance electrolyte wettability as well as the electrode conductivity.

Another relationship is indicated in Fig. 10, where it is shown that high-rate discharges at −40 °C can improve subsequent performance in lower rate discharging at the same temperature. Fig. 10(a) shows that an initial $C/20$ rate discharge yields about 150 mAh g^{-1} of capacity in a Li/$CF_{0.647}$ cell. Fig. 10(b) indicates that if a very short $C/10$ rate discharge preceded a $C/20$ discharge, over 500 mAh g^{-1} was extracted for this similar cell. There is a voltage recovery event early on in this $C/20$ discharge, which may also be indicative of a variety of possible electrode conditioning effects. In other cases, significantly more capacity was extracted at a $C/10$ rate at −40 °C, as in Fig. 10(c). The exact causes of these variations are not known and are currently under study. Early results are consistent with the idea that

the increased electrolyte viscosity at low temperatures disallows uniform electrode surface wetting, thereby resulting in a fluctuating (sometimes to catastrophic levels) discharge potential. Data from cells using a lower viscosity electrolyte display more consistent behavior [11].

5. Conclusions

This work shows that the nano-scale intermixing of graphitic domains and CF_y found in sub-fluorinated CF_x (SFCF$_x$) materials greatly benefited the specific capacity of these materials when discharged at low temperatures using aggressive current densities. The performance of SFCF$_x$ materials was compared to industry-standard, fully fluorinated $CF_{1.08}$ powders inserted in otherwise identical test cells. The SFCF$_x$ and $CF_{1.08}$ active material yielded nearly the same specific capacity values at room temperature at rates as high as $2C$. However, the SFCF$_x$ gave a three times (or greater) capacity value at −40 °C using rates up to $C/10$. The results also indicate that a room-temperature pre-discharge is critical to low-temperature performance, an effect attributed to the kinetically motivated cathode depassivation/conditioning events that occur upon initial discharge. It is suggested that the pre-discharge results in the evolution of a fluorine-free C layer at the electrode/electrolyte interface that would subsequently enhance electrolyte wettability and conductivity. These results show that the high specific capacity SFCF$_x$ cathode chemistry is a viable intermediate rate low-temperature battery cathode material if prepared in a sub-fluorinated state and implemented in a sufficiently thin-electrode cell design. Future work is dedicated to optimizing the electrolyte content for low temperature performance.

Acknowledgements

References

[1] G. Bruce, Development of a CF_x D cell for man portable applications, in: Proceedings of the Joint Service Power Expo, 2005.
[2] J.P. Gabano, in: M. Fukuda, T. Iijima (Eds.), Lithium Batteries, Academic Press, New York, 1983.
[3] D. Linden, T.B. Reddy, Handbook of Batteries, 3rd ed., McGraw Hill, New York, 2001.
[4] R.G. Gunther, Proceedings of the Fifth Power Sources Conference, 1975, pp. 713–728.
[5] T. Tan, P. Lam, H. Yumoto, Li/(CF)$_n$ battery for low temperature and high power application, in: Proceedings of the 208th Electrochemical Society Meeting, Los Angeles, CA, 2005.
[6] D. Rohde, M.J. Root, D. Fostor, Li/CF_x cell and material development for high rate applications, in: Proceedings of the 37th Power Sources Conference, 1996.
[7] P. Hany, R. Yazami, A. Hamwi, J. Power Sources 68 (2) (1997) 708–710.
[8] P. Lam, R. Yazami, J. Power Sources, 2005.
[9] Y. Kita, N. Watanabe, Y. Fujii, J. Am. Chem. Soc. 101 (14) (1979) 3832–3841.
[10] F. Walsh, M. Pozin, J.K. Tikhonov, Storage of Li/CF_x cells, in: Proceedings of the 38th Power Sources Conference, 1998.
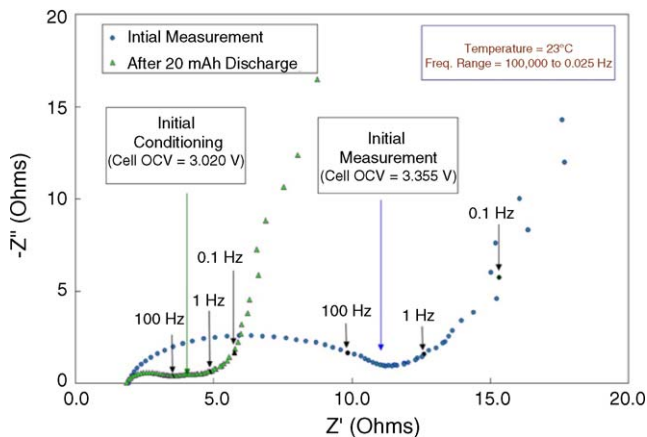[11] Whitacre, et al., in press.

Fig. 13. Electrochemical impedance spectroscopy data from the cathode side of a three electrode Li–$CF_{1.08}$ test cell before and after a 2 h room-temperature conditioning discharge.